

Cite this: *Phys. Chem. Chem. Phys.*, 2012, **14**, 616–625

www.rsc.org/pccp

PAPER

Spectroscopic characterization of the first ultrafast catalytic intermediate in protochlorophyllide oxidoreductase†

Olga A. Sytina,^{‡a} Ivo H. M. van Stokkum,^a Derren J. Heyes,^b C. Neil Hunter^c and Marie Louise Groot^a

Received 26th May 2011, Accepted 25th October 2011

DOI: 10.1039/c1cp21713e

The enzyme NADPH:protochlorophyllide oxidoreductase (POR) catalyses the reduction of protochlorophyllide into chlorophyllide, a precursor of chlorophyll *a* in photosynthetic organisms. The enzyme binds the substrate and the cofactor in the dark and catalysis is initiated by the absorption of light by the substrate. We have carried out spectroscopic measurements with ultrafast time resolution under single pulse conditions, which reveal a biphasic formation of the first catalytic intermediate, I675* with average rates of $(3.7 \pm 0.7 \text{ ps})^{-1}$ and $(177 \pm 78 \text{ ps})^{-1}$, as obtained from a systematic analysis of 15 datasets. Measurements in the mid-IR absorption spectral region show that I675* is associated with a decrease of the PChlide C=O keto oscillator strength. The spectroscopic changes in the visible and mid-IR regions are specific for the enzyme reaction as they do not occur in the photoexcited substrate alone. In deuterated samples, the rates of I675* formation are reduced by a factor of 1.5–2 compared to protonated samples, suggesting the involvement of a proton movement in this reaction step. The quantum yield of this step is determined to be 0.64 ± 0.11 , and the quantum yield of the final reaction product formed on a later time scale, chlorophyllide, is 0.26 ± 0.06 . Several possible interpretations of these data are discussed.

Introduction

The enzyme protochlorophyllide oxidoreductase (POR), from the family of short-chain alcohol dehydrogenases, catalyses the conversion of protochlorophyllide (PChlide) into chlorophyllide (Chlide), upon the absorption of light. This is an important regulatory step in chlorophyll biosynthesis and the subsequent assembly of the photosynthetic apparatus. It is proposed that a conserved tyrosine residue of the enzyme donates a proton to the C18 position and a hydride is transferred from the *pro-S* face of the NADPH nicotinamide ring to the C17 position of the PChlide molecule¹ (see the inset in Fig. 1). Usually, the rate of a biological reaction is limited by the relatively slow, diffusion-dependent binding of a substrate, and a proton transfer reaction does not always lead to a clear spectroscopic change. However, in POR the formation of

the enzyme–substrate complex in the dark prior to illumination² is a way to remove slow diffusion limited binding and release events from the experiment and provides a doorway to follow fast proton and electron transfer processes in real-time.^{3,4} Hence, the requirement of light for the initiation of catalysis by POR makes this enzyme an excellent model system for studying the mechanisms and timescales of enzyme-mediated proton and hydride transfers, including questions related to the involvement of tunnelling, the nature of the driving force and the relation to short- and long-range protein motions.^{5–9}

The enzyme can occur in a catalytically inactive or active state, and inactive enzymes are activated by absorption of a photon by the substrate. Time-resolved transient absorption measurements revealed a highly non-linear light dependency of the Chlide accumulation, upon increasing illumination.⁴ We showed that upon the absorption of a first photon, the enzyme complex undergoes a structural change that has a distinct spectroscopic signature in the mid-IR region, whereas catalysis occurs upon absorption of a second photon. The lifetime of the active POR conformation is long and survives turnover.⁴

The initial step in catalysis proceeds on an ultrafast timescale and results in the formation of the intermediate I675*. The I675* intermediate is characterized by stimulated emission at 675 nm, red shifted by 30 nm from that of POR-bound PChlide, and the precise nature of this state has remained undetermined. The 30 nm red shift is larger than that occurs

^a Department of Physics and Astronomy, Faculty of Sciences, VU University, De Boelelaan 1081, 1081 HV Amsterdam, The Netherlands

^b Manchester Interdisciplinary Biocentre, University of Manchester, 131 Princess Street, Manchester M1 7DN, UK

^c Department of Molecular Biology and Biotechnology, University of Sheffield, Firth Court, Western Bank, Sheffield, S10 2TN, UK

† Electronic supplementary information (ESI) available. See DOI: 10.1039/c1cp21713e

‡ Current affiliation: FOM Institute AMOLF, Science Park 102, 1098XG, Amsterdam, the Netherlands, sytina@amolf.nl

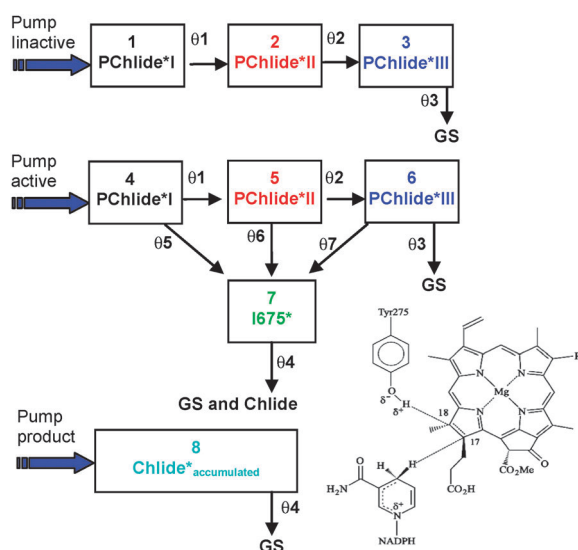


Fig. 1 Kinetic scheme used in target analysis of the illumination-dependent POR transient absorption datasets. Each compartment in the scheme is characterized by Species Associated Difference Spectra (SADS). The transition rates between spectral compartments are free parameters in the target analysis. The rates are not allowed to vary from scan to scan, because physically, transition rates are not light-dependent parameters. Instead the relative concentrations of inactive, active and accumulated products were assumed to depend on the scan number. In order to reduce the number of free parameters a number of spectral constraints were implemented. A substrate bound to an active enzyme and a substrate bound to an inactive enzyme were set to be spectrally undistinguishable, *i.e.* $SADS_1 = SADS_4$, $SADS_2 = SADS_5$, $SADS_3 = SADS_6$, thus the total number of SADS was reduced from 8 to 5.

for PChlide in methanol upon formation of the excited state, where strengthening of a hydrogen bond to the PChlide keto carbonyl group, driven by the internal charge character of the excited state,¹⁰ results in red-shifted fluorescence peaking at 646 nm.^{11,12}

Hydride transfer from NADPH to the substrate was found to occur with a time constant of 0.5 μ s as revealed by a NADPH/NADPD kinetic isotope effect (KIE) in the rate of formation of an intermediate absorbing at 696 nm.^{13,14} In the same study, a subsequent solvent KIE on a time constant of 40 μ s, leading to a 680 nm absorbing intermediate, was assigned to proton transfer from the tyrosine donor to the PChlide molecule. By combining studies of the temperature and isotope dependence of the rate of PChlide reduction it was shown that both H-transfer reactions proceed by using quantum mechanical tunnelling coupled to specific motions (vibrations) in the protein.¹³ Further studies on the role of the bulk solvent in catalysis suggested that solvent-slaved motions control the 40 μ s proton tunneling process but not the hydride tunnelling, implying that a long-range 'dynamic network' from solvent to the enzyme active site, or conformational changes are required to facilitate proton transfer.^{15,16}

The involvement of the PChlide excited state in the catalytic reaction implies that a stable reaction intermediate must be formed within the \sim 2 nanosecond lifetime of the PChlide excited state, in order to preserve the reaction energy. The I675* state can therefore represent such an intermediate, capable of

storing a significant fraction of the excitation energy, to drive the subsequent reactions. DFT calculations¹³ have the first stable intermediate formed directly from the excited state, with the first transfer process involving the hydride H^- , and the proton transferred in the subsequent step.

Here, in order to investigate the nature of I675* in more detail, we compare the rates of the I675* formation for protiated and deuterated samples, and observe light-induced absorption changes in the mid-IR spectral region associated with structural rearrangements during the course of the catalysis. Experiments were performed under single-pulse conditions, in order to separate the effects of the first activating photon from the second, catalytic photon. We apply a target kinetic model adapted for non-cyclic reactions to estimate the quantum yield of the intermediate product I675*, the quantum yield of the final product Chlide, and of the activation process for each dataset. In total we performed measurements on 17 samples under various experimental conditions, to estimate the variation of these parameters in the different experimental sessions involving this complex enzyme. We further compare the effect of blue (475 nm) and red (640 nm) excitations since this was shown to lead to different transient absorption dynamics in isolated PChlide:¹¹ excitation in the Soret band causes a rise of blue shifted stimulated emission signals in transient absorption and a gain of emission in the time-resolved fluorescence, which may interfere with the I675* dynamics due to internal conversion from the S2 to S1 excited states of PChlide on the 700 fs timescale.¹¹

Materials and methods

Sample

PChlide was extracted from *Rhodobacter capsulatus* ZY5, as described previously.¹⁷ Thermophilic *Thermosynechococcus elongatus* BP-1 was overproduced in *E. coli* and purified as previously described.¹⁸ The samples containing 0.5 mM PChlide, 0.5 mM POR and 2.5 mM NADPH in activity buffer (50 mM Tris pH 7.5, 100 mM NaCl, 1% Genapol, 0.1% β -mercaptoethanol) were premixed and kept in the dark at all times before the experiment. For the kinetic isotope effect (KIE) measurements POR was deuterated by exchange into a deuterated buffer, containing 50 mM Tris pH 7.5, 100 mM NaCl, 1 mM DTT. Most samples were sonicated on ice before experiment to enhance binding of PChlide to POR.

Experimental design adapted for a non-cyclic reaction

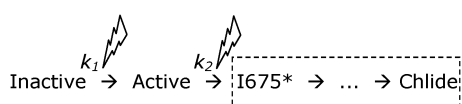
The laser setup has been described previously in more detail.¹⁹ The POR:PChlide:NADPH complexes were excited with 85 fs laser pulses, either at the red edge of the Soret band (S2–S0 transition) of PChlide at 475 nm where the absorption of the product Chlide is minimal, or at 640 nm which corresponds to the absorption maximum of PChlide bound to the protein.^{14,20} To measure the light-induced spectroscopic changes associated with the non-cyclic reaction of the POR enzyme, the samples were held in a Lissajous sample scanner in a 200 μ m cell.¹⁹ The scanner is designed in such a manner as to excite a fresh area of the sample with each next laser pump pulse, which arrives at a rate of 500 Hz. The sample cell is continuously moved in a

plane perpendicular to the laser pump and probe beams. The laser excites the sample along the Lissajous trajectory and approximately after one minute returns to the same sample volume. Such cycle is defined as one sample *scan*. During one scan a full time-resolved spectrum was collected, which later in the text was referred as *single dataset*, or *dataset*. Therefore, the very first sample scan was recorded on a sample that had never seen light, the next sample scan was recorded on a sample a fraction of which had seen one photon already, and may absorb a second photon, the third when a fraction of the sample had seen two photons already, and so on. Thus, despite some degree of heterogeneity due to the illumination pattern of the Lissajous scanner (Fig. S1, ESI†), by choosing a low excitation power we could observe a gradual accumulation of a photoproduct with increasing number of sample scans, in addition to the dynamics of each scan on the pico- and nanosecond time scale. Datasets, corresponding to the consecutive scans, which did not reveal significant differences in spectra and kinetics were averaged together in order to obtain a higher signal-to-noise ratio. Finally such consecutive averaged datasets constitute a series of scans for analysis, and are later in the text referred to as *composite datasets*. The details and structure of averaging can be found in ESI† in Table S2, S3. Steady state absorption spectra were recorded using a Perkin Elmer spectrophotometer (Lambda 40UV/VIS).

Kinetic analysis of a non-cyclic reaction

We applied global analysis^{4,21} for the initial characterization of the time resolved dynamics. The spectral evolution in the absorbance difference spectrum in each dataset can be fitted with a sum of sequentially evolving exponential components, and the amplitudes of these exponential decays are estimated, resulting in so-called evolution-associated difference spectra, EADS.²¹ The time-resolved datasets in all experiments were well fitted with a sum of either three or four exponential components, with increasing lifetimes, and thus decreasing rates. For further and more quantitative characterization of the time- and illumination dependent dynamics and enzymatic activity in each scan we applied a target model, described before,⁴ as depicted in Fig. 1.

The structure of this kinetic target model is based on a phenomenological description of the data. There are several absorbing and emitting species in the sample solution, with illumination-dependent and time-dependent concentrations, *i.e.* PChlide bound to enzyme, PChlide unbound, Chlide accumulated and intermediate catalytic product being formed in the sample scan. The POR-bound population is divided into a fraction of inactive and active enzyme complexes, which obey the dependence on the number of scans in the following sequential manner:



with parameters k_1 —probability of excitation per unit time or, excitation density and $k_2 = k_1 Q$, where Q is the quantum yield of Chlide formation. Solving the associated differential equations leads to an analytical expression for the dependence of these

fractions on the number of sample scans, *i.e.* the number of absorbed photons. This model is referred to as *analytical* and is used for fitting series of many sample scans. In order to fit a single sample scan we modified this model, allowing the fractions of inactive and active enzymes, and accumulated Chlide to be free parameters. This model is referred to as *free*. In both models it is supposed that inactive enzymes do not form any product (branch 1 \rightarrow 2 \rightarrow 3 \rightarrow GS), but active enzyme complexes (branch 4 \rightarrow 5 \rightarrow 6 \rightarrow GS) can form the I675* intermediate, and consequently Chlide. The quality of the fit with global and target analysis was judged by inspection of the singular vectors of the matrix of residuals, which have to be structureless.⁴

Results

Spectroscopic signatures of Chlide formation

The visible absorption spectrum of the POR:PChlide:NADPH complex in the 400–800 nm region is determined by the electronic transitions of the chromophore, either bound or unbound to the protein. A typical absorption spectrum (Fig. 2A) displays the Soret band at 444 nm, and the Q_X and Q_Y bands of the substrate and the product. The band belonging to the unbound substrate, *i.e.* free PChlide in solution, is usually found at 630 nm, the effect of binding to the protein shifts this band towards 640 nm. The relative intensity of the 640 nm band with

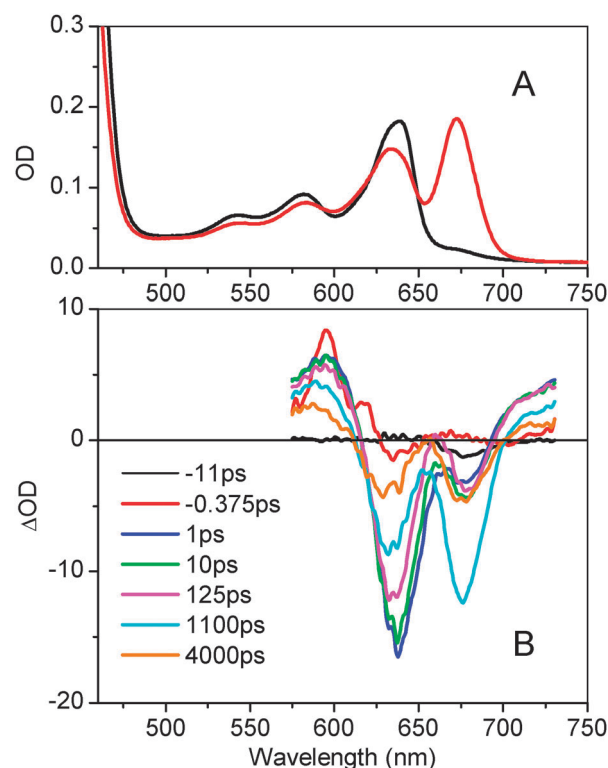


Fig. 2 (A) Absorption spectrum of POR:PChlide:NADPH solution measured in a 1 mm cell before (black) and after illumination (red). (B) Selection of the transient absorption spectra at -11 ps and -0.375 ps before excitation and 1, 10, 125, 1100, and 4000 ps after excitation. The data are the average of scans 7–12, and have not been dispersion corrected.

Table 1 Kinetic parameters estimated in the target analysis of 13 composite datasets (KIE data are not included). The lifetimes (rates⁻¹) of spectral compartments are shown in picoseconds. The parameter $\theta 7$ was estimated in the models as 0. Parameter k_1 is excitation density, parameter QY of Chlide is calculated as k_2/k_1 , where k_2 is derived from the analytical model for the Active \rightarrow Product mechanism. The expression for quantum yield QY of I675* formation is given in the Discussion section

Parameter	$\theta 1^{-1}$ / ps	$\theta 2^{-1}$ / ps	$\theta 3^{-1}$ / ps	$\theta 4^{-1}$ / ps	$\theta 5^{-1}$ / ps	$\theta 6^{-1}$ / ps	k_1	QY of I675*	QY of Chlide
Mean	6	350	2700	2500	10	360	0.10	0.64	0.26
St. dev.	1	200	1040	1050	2	100	0.06	0.11	0.06

respect to that at 630 nm is directly proportional to the fraction of the bound substrate. A sample solution containing an enzyme, substrate and cofactor that has never seen any light is flat in the region above 650 nm. Upon visible illumination the absorption spectrum is modified due to the reduction of PChlide into Chlide: a distinct Q_Y band of Chlide appears at 670–675 nm while PChlide absorption at 630–640 nm is reduced.

Typical time-resolved spectra, obtained by averaging a few single datasets, corresponding to the subsequent sample scans, are shown in Fig. 2B. After absorption of the laser pulse a negative band at 640 nm appears, corresponding to bleached ground state absorption (GS) and stimulated emission (SE) of the PChlide substrate. Because the sample in Fig. 2B had absorbed some light already, at time zero a second negative band at 675 nm appears, corresponding to GS bleach and SE of the product Chlide*, excited by the laser pulse. In a completely dark-kept sample, the signal above 650 nm is positive due to excited state absorption (ESA) of the substrate PChlide*.⁴ The negative signal at 675 nm that appears after time zero originates from SE of the I675* state being formed.

For the analysis we generated 15 composite datasets consisting of many consecutive scans with gradually changing dynamics and spectra,⁴ (see Fig. S2 (ESI[†]) for a set of time traces for different scans) measured on 37 fresh sample preparations. A simultaneous target analysis of consecutive scans was found to be the best possible way to characterize the multi-dimensional data in more detail. The large number of experiments allows us to estimate the variation in the kinetic parameters, *i.e.* rate constants, fractions of active and inactive enzymes, and quantum yields of the intermediate and final products, which are collated in Table 1. The SADS estimated in the target analysis are shown in the ESI[†].

To illustrate that the complex kinetic model of Fig. 1 is needed to obtain a good fit of the data, we tested the hypothesis that all enzymes are active in all scans and data were fitted only to the active branch of the kinetic scheme. The reduced model resulted in a significant misfit of the data (Fig. S2B, ESI[†]), as compared to the quite acceptable fit obtained with the “full” model (Fig. S2A, ESI[†]), where photon flux-dependent inactive and active fractions are allowed.

Spectral dynamics upon blue and red excitation

In Fig. 3 we compare the dynamics of the POR:PChlide:NADPH complex using blue (475 nm) or red (640 nm) excitation. The blue wavelength excites the enzyme complex in the red edge of the PChlide Soret band, whereas the red wavelength excites the Q_Y transition of PChlide. The data from both experiments were analyzed with both analytical and fractional target models (see Materials and methods). Despite the complexity of the kinetic models, realistic and physically meaningful spectra and rates were obtained from the target analysis (Fig. 3, for more see Fig. S3, ESI[†]). The black, red and blue SADS are consistent with bleach and stimulated emission of excited

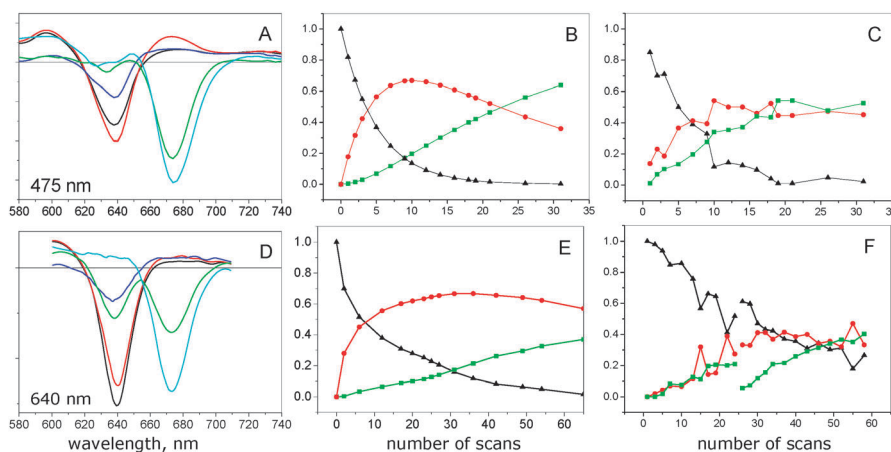


Fig. 3 Comparison of the effect of the excitation wavelength (A, D) on the POR dynamics, and merits of analytical and free target models (B,C,E,F) in two composite datasets. (A) SADS estimated from the target analysis using the analytical model for the 475 nm dataset. (B) Relative concentrations of inactive(▲) \rightarrow active(●) \rightarrow Chlide (■) estimated from the target analysis using the analytical model for the 475 nm measurement. (C) Relative concentrations of inactive(▲) \rightarrow active(●) \rightarrow Chlide (■) estimated from the target analysis using the free model for the 475 nm measurement. (D) SADS estimated from the target analysis using the analytical model for the 640 nm measurement. (E) Relative concentrations of inactive(▲) \rightarrow active(●) \rightarrow Chlide (■) estimated from the target analysis using the free model for the 640 nm measurement. (F) Relative concentrations of inactive(▲) \rightarrow active(●) \rightarrow Chlide (■) estimated from the target analysis using the free model for the 640 nm measurement. Discontinuities in fractions in this case originate from a ‘dark’ break in the experiment. Here, the Lissajous scanner with the sample was stopped and all laser and background illumination was off during 30 minutes, after that the measurement was continued in the same way. After the break the amount of Chlide is reduced slightly due to diffusion in the sample cell during the break.

PChlide (compartments 1–3, 4–6). The green SADS corresponds to the population of compartment 7, *i.e.* represents pure spectra of the first catalytic intermediate I675*, which is formed in the excited state and thus appears as a negative band at 675 nm. The negative band at 635–640 nm in the green SADS corresponds to loss of PChlide absorption due to photoconversion into I675*. The cyan SADS corresponds to the accumulated Chlide product and appears as a negative band at 670–675 nm at time zero.

There is a difference in intrinsic PChlide* dynamics (black, red, blue SADS) when either 475 nm or 640 nm excitation is used. In the case of blue 475 nm excitation, the initial black spectrum evolves into a more intense red spectrum, whereas a gradual decrease from black to red is observed upon direct excitation of the Q_Y at 640 nm. The effect of emission gain upon Soret excitation has been observed in neat PChlide solutions as well, where it was shown to be related to emission from the vibrationally hot molecule, which blue shifted upon cooling, in combination with a relatively slow S₂ to S₁ relaxation time.¹¹

Using the composite datasets we also compare the merits of the analytical and free target models. In the free target model the scatter in fractions with increasing scan number partly arises from too large a freedom in the fit. In addition, using the free model it is usually more difficult to obtain physically reasonable spectra. This problem is overcome in the amplitude target model, where the imposed gradual sequential mechanism: inactive → active → product leads to a reduction in the number of free parameters. In this way the analytical model also allows minimalization of the effect of heterogeneity across the sample and the resulting scatter in the fractions. However, the analytical model lacks the advantage of the free model to fit single datasets and discontinuities in fractions (Fig. 3). From Fig. 3F it is apparent that in the free-fitted 640-nm dataset there is a rather long-lived presence of inactive POR, which could be an indication of unbound PChlide, either relatively more excited at this wavelength, or more present in the sample used for the 640 nm experiment. We discuss this effect in more detail in the Discussion section.

Kinetic isotope effect measurements

In order to determine whether a kinetic isotope effect upon H/D exchange is present, we collected data for samples in H₂O and in D₂O activity buffers. The steady state absorption spectra of samples in both buffers were identical.

An accurate conclusion about a change in the rate of the reaction can be made only if the measurements are performed under identical conditions where the same excitation power and optical alignment are used. Therefore, we analyzed the kinetics of Chlide formation for 6 datasets (3 in H₂O and 3 in D₂O) recorded on the same day, under identical experimental conditions, using the free target model, since the datasets consisted of single scans acquired after a CW illumination for 5 min, in order to get sufficient statistics without optical misalignments.

The traces of transient absorption recorded at 670 nm in H₂O and in D₂O (Fig. 4) show an evident difference in the kinetics. Initially, the traces showed a 5–10% difference in the amplitudes of the negative signals at time zero delay, probably due to a minor difference in the illumination time. After performing

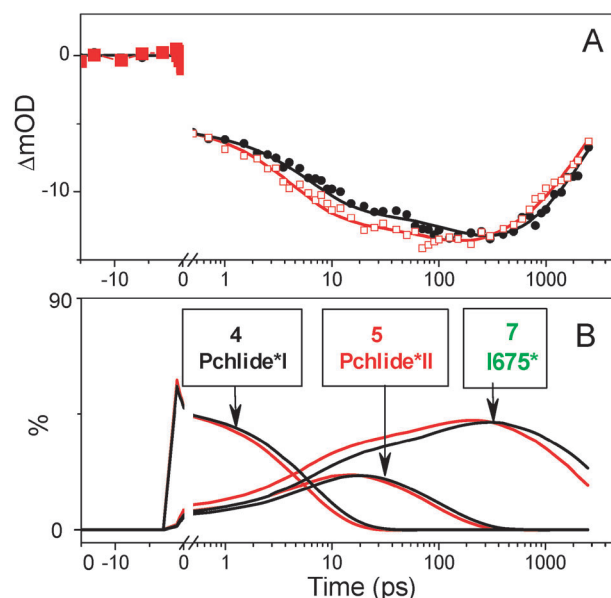


Fig. 4 (A) Solvent effect on the TA dynamics of the POR:PChlide:NADPH complex in two solvents at 670 nm: H₂O (□ red), and in D₂O (● black). Fit of the data resulting from the target analysis is shown by solid lines. (B) Solvent effect on the time profiles of active fractions and intermediate product state I675* in the two solvents.

target analysis the traces have been normalized to better show the different kinetics. The kinetics can be attributed to the gain of SE due to formation of I675*, followed by recovery of I675* and of directly excited Chlide to the ground state. Comparison of the traces in H₂O and D₂O reveals faster appearance of the negative signal of the I675* SE in H₂O than in D₂O. Target analysis was applied to fit all datasets simultaneously to the same kinetic scheme (Fig. 1), in which the rates in the unproductive branch were restricted to be identical in both solvents and independent of H/D exchange (*i.e.* $\theta_1, \theta_2, \theta_3, \theta_4$), whereas the rates of product formation θ_5, θ_6 and θ_7 were allowed to vary for the different solvents. All fractions were free parameters in the model. It was assumed that the corresponding species, *i.e.* SADS in both solvents are indistinguishable (not shown). The time constants found in this case were 6.3 vs. 12.2 ps for PChlide*I → I675*, and 51 vs. 169 ps for PChlide*II → I675*, which results in KIE ratios of 2 and 3, respectively. The error for these kinetic parameters was within 10% range. In order to facilitate the fit to converge closer to the average values, found in the series of the other 15 experiments (Table 1), we tested a model with the PChlide*II → I675* time constant in H₂O fixed at 150 ps. In this case, the KIE ratio for PChlide*II → I675* was reduced to 1.38–1.62, depending slightly on the relative fractions assumed for each dataset, and the KIE ratio for PChlide*I → I675* was about 2. A similar good quality of fit was obtained in both cases.

The relative fractions (Fig. S5, ESI†) of productive enzymes in all cases varied between 48 to 63% and a reasonable estimation of the amount of accumulated Chlide between 18 and 38% was found in all tested models, while the fraction of unproductive enzymes varied between 1 and 27%. We checked that the variation in the fractions did not affect the rates of I675* production and therefore, we exclude that the observed

isotope effect on the rates of PChlide*I (θ_5) and PChlide*II to I675* (θ_6) is due to an error in determining the active and inactive fractions. The variation in these fractions can be explained by the slightly different time of initial CW illumination and variations in the initial concentrations, since several stock sample preparations were used in the experiment. From the target fit of composite datasets (see Fig. 3 and S3, ESI†) it is clear that the highest relative amount of productive enzymes, roughly between 50–60%, can correspond to a very wide range of concentrations of unproductive enzymes and Chlide, depending on the amount of previous illumination (see for example Fig. 3 and S3, ESI†). Therefore, the simultaneous fit of several single datasets with different amounts of illumination is a difficult task, which results in slightly different rates of I675* formation from the typical ones found in the analysis of a series of sample scans.

In the POR reaction mechanism there are two proton donors, which can be replaced by a heavier isotope deuterium (Fig. 1). In the experiment with protiated and deuterated enzymes a difference in the rates of the I675* formation is demonstrated, which suggests that proton movement is involved in this reaction step.

For control we performed experiments on samples in which the second proton donor was replaced with deuterium, *i.e.* protiated enzymes in combination with NADPD were compared to protiated enzymes with NADPH. The analysis revealed that all SADS and fractions profiles are in line with other datasets, however no evident difference in kinetics was found (data not shown). The absence of a KIE on the rate of the I675* formation when NADPD is used is in line with the observed rate of hydride transfer from NADPH with a time constant of 0.5 μ s.

Mid-IR transient absorption spectroscopy

We further measured the TA dynamics of the POR:PChlide:NADPH complex in the 1800–1590 cm^{-1} spectral region, over a –15 ps to 3 ns time range, upon excitation at 475 nm. The more limited signal to noise ratio in the mid-IR excluded the analysis of single scans and therefore we performed a global analysis on the averaged dataset. The data were best fitted to a sequential model with four increasing lifetimes of 0.7 ps, 8 ps, 210 ps and a component longer than the time window of our experiment (Fig. 5). The negative bands at 1735 cm^{-1} and between 1700 and 1650 cm^{-1} correspond to ground state bleachings of the ester and keto groups of the excited chromophores respectively.^{4,11,22} The most intense negative signal appears to be composed of three bands at 1690 cm^{-1} , 1680 cm^{-1} and 1658 cm^{-1} . A broad structureless positive signal, originating from the keto group in the electronic excited state, is observed at 1650–1590 cm^{-1} and a relatively weak positive signal is also present at 1725–1700 cm^{-1} .

To emphasize which dynamics and spectral features are specific for PChlide bound to the enzyme and catalytic conversion, we overlaid EADS of free PChlide in D_2O buffer (Fig. 5). These spectra show a double peaked negative band with maxima at 1695 cm^{-1} and 1682 cm^{-1} , and a positive signal with fine structure, similar to that in the POR:PChlide:NADPH spectrum, extending down to 1590 cm^{-1} . Obviously the POR:PChlide:NADPH complex shows more dynamics than free PChlide in D_2O buffer. With time constants similar

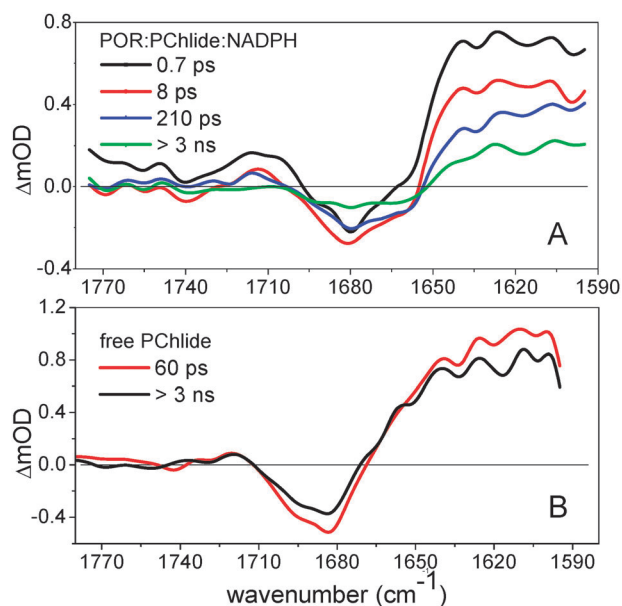


Fig. 5 EADS of the mid-IR TA dynamics: (A) of the POR:PChlide:NADPH complex in D_2O activity buffer pumped at 475 nm; (B) of free PChlide in D_2O activity buffer pumped at 475 nm.

to those observed in the visible spectral region there is a decay of the positive keto induced absorption. The band at 1658 cm^{-1} only appears as a negative band after 0.7 ps, as it is initially obscured by a contribution of excited state absorption, and then remains fairly constant on longer timescales. On a time-scale of 0.7–8 ps the intensity of the positive band decreases, without a concurrent decay in the bleached bands, suggesting that a dynamic change in the keto oscillator strength in the excited state takes place. On the slower timescale of 210 ps further decay of the positive band occurs, which now seems to be accompanied by decay of the bleached signal, suggesting that a partial decay of population takes place.

Discussion

In the present work we have performed transient absorption experiments on the POR-catalysed reaction to validate our earlier model of the catalytic conversion of PChlide into Chlide, involving activation of the enzyme by a first photon and catalytic conversion by a second photon.⁴ In particular, we focused on the nature of the intermediate I675* formed on the picosecond timescale. We now discuss these aspects in more detail.

Kinetic model

From all the collected TA data we can generate the following generic picture of the ultrafast photoreactions in the POR:PChlide:NADPH complex. In order to adequately fit the TA dynamics the total population of POR complexes in the sample needs to be divided into inactive and active fractions, which can convert from inactive to active upon absorption of a photon. The spectral evolution of the inactive fraction, which has never been previously excited with a laser pulse, can be described by the inclusion of three excited states, PChlide*I, II and III, decaying sequentially with rates θ_1 , θ_2 and θ_3 respectively.

In parallel to this process, the active fraction, which has been excited previously with a laser pulse, can form intermediate product I675* from the states PChlide*I and II with rates θ_5 and θ_6 . Both enzyme fractions are spectrally undistinguishable and therefore in the analysis are represented by three spectra, indicated in black, red and blue (Fig. 3). We can reasonably estimate the pure spectra of the first catalytic intermediate I675* (green SADS) and of the accumulated final product Chlide* (cyan SADS). Since the analytical dependence of the fractions of active and inactive enzymes is imposed, the kinetic parameter k_1 —excitation density, characterizing the amount of inactive complexes converted into active after one sample scan, can be independently estimated in the target model. The rate k_2 , associated with Chlide formation, can be estimated from the increase in Chlide concentration as a function of the number of sample scans. It should be noted that k_2 is a convoluted number, determined by the excitation density k_1 , and the quantum yield of Chlide formation. Relative to k_1 , the quantum yield in active enzymes of Chlide formation is on average 0.26 ± 0.06 as obtained from 13 composite datasets measured on 42 fresh sample preparations (including two datasets in D₂O). This estimate for thermophilic POR is in good agreement with that for the Chlide quantum yield in mesophilic POR of 0.21, based on steady-state measurements,¹⁸ and somewhat lower than our previous estimation, based on a single sample preparation measurement.⁴

The quantum yield of the I675* intermediate product in activated enzymes can be calculated using the following expression:

$$\begin{aligned} QY_{I675^*} &= \frac{\theta_{\text{product}}}{\theta_{\text{ex.state}}} = \frac{\theta_{\text{product}}}{\theta_{\text{product}} + \theta_{\text{loss}}} \\ &= \frac{\theta_5}{\theta_5 + \theta_1} + \frac{\theta_1}{\theta_1 + \theta_5} \cdot \frac{\theta_6}{\theta_6 + \theta_2} \end{aligned}$$

where θ_{product} and θ_{loss} refer to the rates towards the I675* state and to the PChlide*II (or PChlide*III) state, respectively, which results in a 0.64 ± 0.11 yield. The catalytic processes converting I675* into Chlide therefore appear to have a yield of $0.26/0.64 = 0.4$ (40%).

Variation in parameters and spectra

In the analytical model, a sequential conversion of inactive POR into active POR, and into a Chlide–POR product is imposed. Where possible we reverted to this model because of the restriction in the parameters and the resulting more estimable spectra it afforded, as well as a handle on physically relevant parameters, such as the quantum yield of each process. However, there are indications that this model does not describe all aspects of the POR catalytic process. Here, we will discuss variations in spectra and kinetic parameters, and to which extent they may be caused by slightly varying experimental parameters and/or provide us with insights into how to refine this model.

We observe variations in spectral shapes and the ratio of accumulated Chlide and newly formed I675* (green and cyan SADS, respectively) in different experiments (samples). The different ratios of Chlide and I675* bands among samples can be caused by the excitation of PChlide and Chlide in different proportions, at the particular excitation wavelength, which

could have varied a few nm (from 475 to 480 nm) between experiments. The amplitude of the SE signal at 675 nm is overall about two times larger than that of the PChlide bleach in the I675* spectrum. This most likely represents an increase in the chlorine extinction coefficient, going from PChlide to the I675* state.

From Fig. 3 and S3 (ESI†) it is apparent that the fraction of accumulated Chlide (cyan spectrum 8) is reasonably independent of the model used. However, the fractions of inactive and active POR appear to vary between experiments and are more dependent on the model used. In the model we do not include a compartment for unbound PChlide molecules, which means that they are effectively included in the inactive POR–PChlide compartment, leading to a deviation in the estimated conversion of inactive into active enzymes. This is even more complicated by processes such as binding of unbound PChlide by turned-over POR enzymes. The inactive and active POR spectrally overlap, and are therefore most affected by neglecting the free PChlide from the models.

If we now see to what extent these variations in the data and modelling have influenced the fitted parameters we find the following: θ_1 , θ_5 and θ_6 have a relatively small standard deviation, whereas θ_2 , θ_3 , θ_4 and k have a large deviation. θ_1 , θ_5 and θ_6 are associated with the formation of I675* (see Fig. 1), either directly *via* PChlide*I, or *via* PChlide*II. This shows we can conclude with confidence that I675* is formed with rates of $\theta_1 + \theta_5 = (3.7 \pm 0.7 \text{ ps})^{-1}$ and $\theta_2 + \theta_6 = (177 \pm 78 \text{ ps})^{-1}$, with a total I675* quantum yield of 0.64. The rates of θ_2 , θ_3 , and θ_4 are the relaxation of PChlide*II to PChlide*III (350 ps), the decay of PChlide*III to the ground state (3 ns) and the lifetimes of I675* and Chlide (2.5 ns, constrained to be equal), respectively.

In pump-probe experiments extending up to 3 ns, as presented here, the determination of lifetimes on the ns timescale is inherently uncertain. In addition, PChlide in solution forms a triplet state on the 1–3 ns timescale, characterized by the loss of the relatively intense PChlide excited state absorption and the stimulated emission.^{11,12} To keep the number of parameters low we did not include this in the target model, but a difference in the triplet yield of inactive or unbound PChlide may have led to a spread in the ns lifetime.

The variation in θ_2 (relaxation of PChlide*II to PChlide*III) representing either loss of stimulated emission,¹¹ or population decay¹² may again be caused by a variation in the contribution of unbound PChlide in the data. If so, it would imply that the dynamics of bound and unbound PChlide are slightly different. As the first scan dynamics representative of inactive POR–PChlide complexes (bound) tend to show a major decay in intensity on the hundreds of picoseconds time scale, it suggests that the relaxation dynamics of bound PChlide tend to be more in the 500–700 ps range, and relaxation of unbound PChlide in the 100 ps time range. We found that for the isolated, unbound PChlide in (i) buffer solution (no enzyme present), the relaxation dynamics in the mid-IR on the ps–ns time scale could be described by a minor 60 ps process and a 1.5 ns excited state lifetime,¹¹ and (ii) THF, isolated unbound PChlide shows a decay of the red side of the negative TA signal, associated with SE, with a 10 ps time constant, followed by major decay of the band with a 900 ps time constant.¹¹ It suggests that the excited

state lifetime of unbound PChlide is long, but a loss of some stimulated emission occurs on shorter tens of picoseconds time scale.¹¹ Similarly here the decay of unbound PChlide* spectra I to II to III in the 650–660 nm region is an indication of the loss of stimulated emission.

A difference in intrinsic PChlide* dynamics (black I to red II to blue III evolutions) is observed when either blue (475 nm) or red (640 nm) excitation is used. The effect of emission gain upon blue excitation is observed also in experiments on isolated, unbound PChlide solutions and is a consequence of exciting with excess energy in the Soret transition.¹¹

Despite the overall complexity of the experiment and the approximation used in the modeling, the kinetic scheme adequately describes the most essential processes in the enzymatic reaction. A good combination of PChlide to POR ratio and a choice of an excitation wavelength optimally selective for bound PChlide can help to minimize some of the sources of uncertainties in this experiment. Furthermore, experiments on the 1 ns to 1 microsecond would help to follow the fate of I675 upon return to the ground state, as well as to determine the relative contribution of triplet formation in the different complexes.

Ultrafast mid-IR dynamics in POR

The timescale of the mid-IR TA experiment overlaps with the TA measurements in the visible region, however information regarding scan-dependent changes in the mid-IR dynamics, corresponding to the one, two and three photon processes, is not available because consecutive sample scans needed to be averaged together in order to achieve a satisfactory signal-to-noise ratio. The time constants (0.7, 8 and 210 ps) from global analysis of the mid-IR TA dataset are in a good agreement with the visible TA experiment.

In the mid-IR TA experiment we expect the dynamics of bound and unbound PChlide and accumulated Chlide rather than protein signals, because we assume that the 3 ns time range does not overlap with the time range of induced conformational changes in POR, registered by the FTIR method.^{4,22} Hence, the negative signals in the mid-IR TA spectrum originate mainly from the ground state absorption of free and POR-bound PChlide and Chlide, whereas the positive signals are likely to belong to vibrations of chromophores in the electronically excited state, and to the intermediate catalytic product I675*, which is formed on the ps timescale upon excitation of bound PChlide. A difference signal from NADPH/NADP⁺ should not be present in these data, as previous measurements on the micro-/millisecond timescale have shown that the hydride is transferred with a rate constant of 500 ns⁻¹, which is far beyond our 3 ns range.¹³ Consistent with this, we do not observe, on any timescale, a bleaching of a band at 1688 cm⁻¹ or a positive absorption appearing at around 1670 cm⁻¹, as we would expect for the hydride transfer reaction from NADPH according to previous assignments.²² It was also established in previous FLN experiments²² that the keto mode of bound PChlide is located at 1653 cm⁻¹, for unbound PChlide in buffer solution it is upshifted to 1682 cm⁻¹, and the keto mode of Chlide is located at 1668 cm⁻¹.

The TA mid-IR spectra of the POR complex show the presence of three negative bands, at 1658–1656 cm⁻¹, ~1680 cm⁻¹ and ~1690 cm⁻¹, thus suggesting the three contributions of bound

and free chromophores. Since we excluded the keto mode of cofactor NADPH, these may originate from free and bound PChlide and Chlide, which all can be excited with the 475 nm pulse. The 1690 cm⁻¹ band in the POR spectra overlaps quite well with one of the bands present in free PChlide in D₂O buffer. Hence, this band probably belongs to unbound PChlide, and possibly, the broad induced absorption of this keto band partially obscures the expected bleach at 1653 cm⁻¹ for bound PChlide. Comparison of the induced absorption in the POR complex and free PChlide suggests that this cancellation is quite effective.

The induced absorption in free PChlide does not show a downshift and decay to such an extent as in the POR complex on similar timescales. Instead, in D₂O-buffered solution a behavior similar to that of PChlide in organic solvents (methanol, THF)¹¹ is observed. Therefore, we conclude that the induced absorption dynamics in the 1650–1590 cm⁻¹ region in the POR complex are associated with formation of the I675* catalytic product, rather than with the dynamics of free PChlide and/or Chlide. The decay of induced absorption is accompanied by a persistent bleach of the negative 1658–1656 cm⁻¹ band, which thus is consistent with the assignment to bound PChlide being converted to I675*.

The mid-IR TA data demonstrate that the catalytic conversion process appears to be reflected in the dynamics of induced absorption of the PChlide keto, which is located in proximity to the reactive site. Consequently it may be sensitive to electronic changes accompanying or preceding the catalytic chemistry. Any structural alterations in the E ring have been shown to disrupt PChlide reduction.²³ The strong decrease in intensity of the keto mode of I675* relative to the PChlide excited state can be explained by a weakening of the C=O dipole moment due to disappearance of the electron density. Alternatively, it may also result from a further strengthening of H-bonding interactions, since the keto of the bound PChlide already has a very strong hydrogen bond with the enzyme residues.²² At the moment it is difficult to interpret these spectra more quantitatively, although the mid-IR TA data clearly demonstrate a correlation between formation of the first catalytic intermediate I675* and the dynamics of the C=O keto group of PChlide.

Kinetic isotope effect measurements

The results of the target analysis of 13 composite datasets (ESI†, Table S1) demonstrate that the appearance of the I675* intermediate in POR proceeds with average rates of $\theta_1 + \theta_5 = (3.7 \pm 0.7 \text{ ps})^{-1}$ and $\theta_2 + \theta_6 = (177 \pm 78 \text{ ps})^{-1}$, with a total I675* quantum yield of 0.64. The time constants are in accordance with those previously reported of 3 ps and 400 ps by global analysis.^{3,4} The first 3 ps process was previously tentatively assigned to the proton transfer from the tyrosine residue of POR to the C18 position of PChlide, and hydride H⁻ transfer, from NADPH to the C17 position of PChlide, was assigned to the 400 ps component.³ In subsequent measurements on much slower timescales, a KIE effect of 2 upon NADPD/NADPH replacement was resolved for formation of the 696 nm intermediate, and a subsequent solvent KIE effect of 2.2 for the appearance of the 680 nm absorbing intermediate, suggesting that the H-transfer reactions occur in a sequential mechanism on the microsecond timescale.¹³ Here, we performed

measurements on the isotope substituted enzyme complexes to test the nature of the early intermediates. Our data now demonstrate a difference in the kinetics of I675* formation on the ultrafast timescale between proton and deuterium substituted samples, which is an indication of the involvement of proton movement in the process. The KIE is about 2 for the first rate, θ_5 , and ~ 1.5 for the second rate, θ_6 . No effect of NADPH/NADPD replacement was observed.

Therefore, we have now the situation that a NADPH/NADPD kinetic effect is observed only on the microsecond timescale for the formation of the 696 nm intermediate, in accordance with hydride transfer taking place after I675* formation, but solvent KIEs are observed both for the formation of the I675* state on the picosecond timescale, and for the formation of the 680 nm state on the microsecond timescale.¹³ We consider two possible scenarios that might lead to a double solvent KIE during the course of the reaction. The first would be that the I675* state corresponds to a tightly hydrogen-bonded PChlide state that is formed after excitation, priming the PChlide for the actual hydride and proton transfer occurring on the microsecond timescale. As tightening of hydrogen bond(s) also corresponds to proton movement, this may result in a KIE effect. However, when PChlide is bound in the active site of the protein it has already formed a strongly hydrogen-bonded complex: binding of PChlide to the protein causes a 10 nm red shift in the absorption spectrum²⁰ and fluorescence line narrowing experiments show that at least the keto carbonyl group of PChlide is downshifted by approximately 50 cm^{-1} when bound to the enzyme, which is clear evidence for a strong hydrogen bonding between PChlide polar residues and protein residues.²² In this case the I675* intermediate corresponds to the formation of additional hydrogen bonds between PChlide and protein residues, or to the rearrangement of H-bond interactions inside the protein active site. Previous DFT calculations have shown that only a relatively small number of additional H-bonding interactions to PChlide can lead to significant red-shifts in the absorption spectrum.¹⁰ On the other hand, it is also possible that formation of the I675* intermediate represents an actual proton transfer reaction, either to the C18 position of PChlide, leading to the formation of the PChlide*-H⁺ and Tyr⁻, or alternatively to the C13 position of PChlide to form an enolate intermediate.²³ If the proton was transferred to the C18 position then the second slow solvent isotope effect on the microsecond timescale can be re-interpreted as the re-protonation of the tyrosine radical by a proton taken up from the solvent. This scenario appears to provide a stable photoproduct that bridges the time-gap between the excited state lifetime and the hydride transfer on the microsecond time scale, explaining how the light-sensitive POR enzyme utilizes the energy of the excited state for catalysis. However, refined calculations of the POR dynamics and further kinetic experiments (possibly on pH dependence) are necessary to choose between these different scenarios.

PChlide* and I675*

The intrinsic PChlide excited state dynamics in several solvents had been investigated previously in order to obtain a better understanding of the PChlide dynamics in POR.¹¹ The dilution of the chromophore in solvents with different electron and

proton donating properties, and of H-bonding interaction strength, is a mimic of the protein environment to some extent. In organic solvents the PChlide electronic excited state has a nanosecond lifetime and decays to the triplet state with a quantum yield of $\sim 23\%$.¹¹ During the excited state lifetime, the stimulated emission is quenched, which was attributed to the solvation of the excited state, which has a mixed internal charge-transfer character.¹⁰ For PChlide in methanol charge transfer state (CTS) formation is facilitated *via* strengthening of the H-bonds and is characterized by appearance of 646 nm emission.¹¹ Here, we have demonstrated that such a state is not formed during enzymatic photoconversion of PChlide, but instead that the I675* catalytic intermediate is formed. The associated spectral change in POR is much larger than observed with strengthening of PChlide H-bonds in solvent,¹¹ implying that the I675* is characteristic of the enzyme reaction only, and the nature of the I675* state is different from the proposed hydrogen-bonded complex.⁴ The formation of the I675* state shows a solvent KIE, implying the involvement of proton movement in this reaction. Such proton movements can significantly change the distribution of electron density around the reactive site of the PChlide molecule, and thus also reduce the C=O oscillator strength *via* reduction of its electrical dipole moment, which is consistent with the mid-IR TA data.

Conclusions

In conclusion, the combination of a convenient model system, such as the light-dependent POR enzyme, with carefully designed kinetic experiments allows the real time observation of catalytic reactions. In a systematic analysis of a large number of datasets we confirm that two forms of enzyme complexes are needed to describe the experimental data. The highly non-linear dependency of product accumulation is caused by a sequential two-photon mechanism, where initially inactive enzyme complexes become active upon absorption of the first photon, whereas the second photon initiates the catalysis. The catalysis in active enzymes starts with the bi-phasic formation of an intermediate in the excited state, I675*, with effective rates of $(3.7 \pm 0.7\text{ ps})^{-1}$ and $(177 \pm 78\text{ ps})^{-1}$, which is further converted into the final product Chlide with $\sim 26\%$ efficiency. By linking the dynamics of isolated PChlide and of PChlide bound to the POR complex we now explicitly demonstrate that the formation of the I675* state is characteristic of the enzyme reaction only. The observation of an ultrafast KIE now continues an important discussion on the catalytic pathway. To determine the catalytic mechanism in detail further kinetic experiments and stronger theoretical support are still required.

References

- 1 N. Lebedev and M. P. Timko, *Photosynth. Res.*, 1998, **58**, 5–23.
- 2 D. J. Heyes and C. N. Hunter, *Trends Biochem. Sci.*, 2005, **30**, 642–649.
- 3 D. J. Heyes, C. N. Hunter, I. H. M. van Stokkum, R. van Grondelle and M. L. Groot, *Nat. Struct. Biol.*, 2003, **10**, 491–492.
- 4 O. A. Sytina, D. J. Heyes, C. N. Hunter, M. T. Alexandre, I. H. M. van Stokkum, R. van Grondelle and M. L. Groot, *Nature*, 2008, **456**, 1001–1008.
- 5 A. Kohen, R. Cannio, S. Bartolucci and J. P. Klinman, *Nature*, 1999, **399**, 496–499.

- 6 E. Z. Eisenmesser, O. Millet, W. Labeikovsky, D. M. Korzhnev, M. Wolf-Watz, D. A. Bosco, J. J. Skalicky, L. E. Kay and D. Kern, *Nature*, 2005, **438**, 117–121.
- 7 P. K. Agarwal, *J. Am. Chem. Soc.*, 2005, **127**, 15248–15256.
- 8 L. Wang, N. M. Goodey, S. J. Benkovic and A. Kohen, *Proc. Natl. Acad. Sci. U. S. A.*, 2006, **103**, 15753–15758.
- 9 L. Masgrau, A. Roujeinikova, L. O. Johannissen, P. Hothi, J. Basran, K. E. Ranaghan, A. J. Mulholland, M. J. Sutcliffe, N. S. Scrutton and D. Leys, *Science*, 2006, **312**, 237–241.
- 10 G. J. Zhao and K. L. Han, *Biophys. J.*, 2008, **94**, 38–46.
- 11 O. A. Sytina, I. H. M. van Stokkum, D. J. Heyes, C. N. Hunter, R. van Grondelle and M. L. Groot, *J. Phys. Chem. B*, 2010, **114**, 4335–4344.
- 12 B. Dietzek, S. Tschierlei, G. Hermann, A. Yartsev, T. Pascher, V. Sundstrom, M. Schmitt and J. Popp, *ChemPhysChem*, 2009, **10**, 144–150.
- 13 D. J. Heyes, M. Sakuma, S. P. de Visser and N. S. Scrutton, *J. Biol. Chem.*, 2009, **284**, 3762–3767.
- 14 D. J. Heyes, A. V. Ruban, H. M. Wilks and C. N. Hunter, *Proc. Natl. Acad. Sci. U. S. A.*, 2002, **99**, 11145–11150.
- 15 G. Durin, A. Delaunay, C. Darnault, D. J. Heyes, A. Royant, X. Vernede, C. N. Hunter, M. Weik and D. Bourgeois, *Biophys. J.*, 2009, **96**, 1902–1910.
- 16 D. J. Heyes, M. Sakuma and N. S. Scrutton, *Angew. Chem., Int. Ed.*, 2009, **48**, 3850–3853.
- 17 D. J. Heyes and C. N. Hunter, *Biochemistry*, 2004, **43**, 8265–8271.
- 18 D. J. Heyes, A. V. Ruban, H. M. Wilks and C. N. Hunter, *Proc. Natl. Acad. Sci. U. S. A.*, 2002, **99**, 11145–11150.
- 19 M. L. Groot, L. van Wilderen and M. Di Donato, *Photochem. Photobiol. Sci.*, 2007, **6**, 501–507.
- 20 D. J. Heyes, G. E. M. Martin, R. J. Reid, C. N. Hunter and H. M. Wilks, *FEBS Lett.*, 2000, **483**, 47–51.
- 21 I. H. M. Van Stokkum, D. S. Larsen and R. Van Grondelle, *Biochim. Biophys. Acta*, 2004, **1657**, 82–104.
- 22 O. A. Sytina, M. T. Alexandre, D. J. Heyes, C. N. Hunter, B. Robert, R. van Grondelle and M. L. Groot, *Phys. Chem. Chem. Phys.*, 2011, **13**, 2307–2313.
- 23 H. Klement, M. Helfrich, U. Oster, S. Schoch and W. Rudiger, *Eur. J. Biochem.*, 1999, **265**, 862–874.